Spreading and bouncing of liquid alkane droplets upon impacting on a heated surface

Mengxiao Qin[1,2], Chenglong Tang[1]*, Yang Guo[1], Peng Zhang[2] and Zuohua Huang[1]

1. State Key Laboratory of Multiphase Flows in Power Engineering, Xi'an Jiaotong University, Xi'an, 710049, People's Republic of China
2. Department of Mechanical Engineering, The Hong Kong Polytechnic University, Hung Hom, Kowloon, Hong Kong

Abstract

This paper reports an experimental investigation on the impact dynamics of liquid normal alkane (n-heptane, n-decane and n-tetradecane) droplets on a stainless steel surface using high speed photography and long distance microscopic techniques and the particular interest is to comprehensively explore the effects of liquid properties, surface temperature, and surface roughness on droplet spreading and bouncing dynamics at different thermal hydrodynamic impact regions. Firstly, high speed images identified four regimes of physical phenomena that couple the droplet spreading hydrodynamics, heat transfer and phase change. Bubbles generation due to the heating of the surface with compression of air disk under the droplet was observed and this phenomenon is firstly promoted and then inhibited with the increase of the wall temperature until finally no bubbles were observed when wall temperature is beyond the Leidenfrost point (T_L). Rim disturbances during spreading were observed at relatively high Weber number and for wall temperature higher than T_L, and increasing wall temperature reduces the rim disturbance. Secondly, the measured non-

dimensional maximum spreading diameter β_{max} decreases with the increase of surface temperature until it becomes a constant when temperature is beyond T_L, and rough surface results in a slightly lower β_{max} than the smooth surface. Finally, for wall temperature beyond T_L, droplet bounces up after a certain period of residence time (τ_r). It takes more time for droplet to rebound at larger We because of larger β_{max} during the spreading. Both surface roughness and liquid viscosity barely influence the τ_{max} but significantly increases the residence time, which haven't been reported in previous models of τ_r and should be considered in the future work of the residence time models.

Key words: droplet impact; high temperature; rough surface; spreading diameter; residence time

1. Introduction

Droplets impacting a heated surface is concerned in combustion engines, spray cooling, and even prevention of blade erosion in gas turbines. The impact phenomenon is significantly complex as it is governed by the coupled physics of heat transfer, phase change and hydrodynamics. Furthermore, the heat transfer rate from surface to droplet is non-monotonic with increasing surface temperature, as shown by the Nukiyama curve. Generally, four regimes in terms of the heat transfer rate have been identified[1-3]. In the droplet evaporation regime where the surface temperature T_w is below the liquid boiling temperature T_b, the impact dynamics is similar to that at cold surface but is affected by the temperature-dependent surface tension. When T_w increases to a value beyond T_b, nucleate boiling occurs and isolated vapor bubbles

generated at the contact surface rise to the liquid air interface; this is called nucleate boiling regime. The heat transfer rate reaches its maximum at a critical heat flux temperature T_C which is also called the "boiling crisis" point. Further increasing surface temperature reduces the heat transfer rate, because the vapor bubbles are populated and merge to form larger ones or even a vapor film so that the droplet partially contacts the surface; this regime is called the transition regime. If the temperature is further increased to above the Leidenfrost temperature, T_L, the stable vapor film prevents the droplet from contacting the solid surface completely so as to reduce the heat transfer rate to a minimum; this is the film boiling regime or Leidenfrost regime.

Although there is general consensus on the sequential occurrence of these four regimes with increasing T_w, most of the previous experiments were performed with a given liquid and surface. As the result, the critical points, such as T_L and T_C on the boiling curve, depend on the impact condition[4]. The transition boundaries of water droplets on heated polished aluminum surface between different impact regimes were discussed by Bertola [5]. Three regimes were identified and transitions between different regimes were discussed by Tran[6].

The maximum spreading diameter of droplet, which is usually normalized by the droplet initial diameter to yield β_m, is critical to droplet impacting a solid surface. Many studies have been devoted to understanding various factors affecting β_m, such as the impact velocity[7], liquid viscosity [8] and surface roughness [9]. Droplet impact in film boiling regime is usually considered to be related to the *We*. Several

correlations have been proposed[6, 10, 11].

As a concomitant quantity of droplet spreading, the residence time, which is defined as the time between the droplet impact on the surface to the droplet rebound from the surface, is also crucial for the heat transfer upon droplet impacting a heated wall. The residence time was found to decease with increasing the impact velocity[9]. The hydrophilic surface treatment was found to remarkably reduce the drop-solid contact angle and results in increased β_m and decreased residence time[12]. The contact time was found almost independent of the impinging angle[7] and impact velocity[7, 13]. The increase of droplet diameter leads to rapidly increased contact time[7]. However, other studies show that residence time was influenced by impact velocity[14].

Surface structure not only influences β_m when the surface is cold but also is important when a droplet impacts a heated surface. Surfaces with micro-structures of different sizes and shapes were found to enhance heat flux during spray cooling. Central jet phenomena was found to occur only on micro-patterned surface[15].

In this work, droplet impact on heated surfaces was experimentally investigated; the alkane droplets have varied liquid viscosity and impact inertia, and the surfaces have different roughness and temperature. Firstly, high speed microscopic techniques will be used to capture the transient impact behaviors at typical thermo hydrodynamic regimes with high time and space resolution such that bubbles generated by the heating of the surface and droplet spreading rim disturbances at varied surface temperature will be examined. In addition, time resolved droplet spreading diameters

with its maximum value for different wall temperature, liquids properties and Weber numbers will be measured for both the smooth and roughed surface. Finally, in the film boiling regime where the wall temperature is higher than the Leidenfrost point, the bouncing height and residence time for droplet at varied surface temperature with different liquid properties are analyzed.

2. Experimental specifications

2.1. Experimental Setup

Figure 1 shows the schematic of the experimental set-up that allows us to observe and distinguish the different regimes of droplets impacting the heated surfaces. The experimental system consists of the droplet generation system, the high-speed imaging system, and the solid surface with temperature control. Droplets are generated at the tip of a hypodermic needle mounted on a three-dimensional positioner and falls down vertically onto the horizontal, dry, stainless steel surface. The droplet impact process was recorded by a Phantom V611 high-speed camera, attached by a long focus microscope and operated at 10,000 fps; the resolution of the recorded video is 100 pixel/mm. The camera is tilted to get more information of the droplet in horizontal direction. The droplet release height H is adjustable, and the velocity before impact can be obtained from the high- speed video. The experiments were conducted in an environment at room temperature (20°C) and atmospheric pressure.
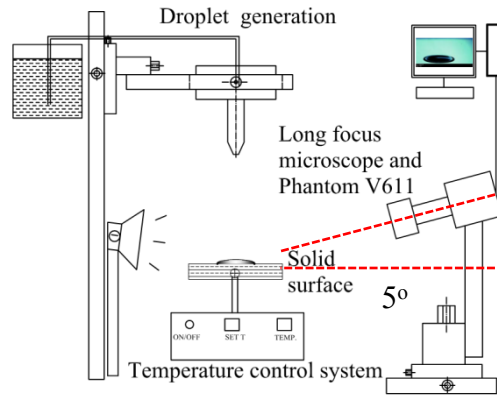
Figure 1 Sketch of the experimental system of droplet impacting a heated surface.

2.2. Characterization of droplets and surfaces

The liquids studied in this work include n-heptane, n-decane and n-tetradecane. The physical properties of these liquid normal alkanes are presented in Table 1. It is seen that the liquids have very similar surface tension coefficients and density but quite different viscosity and boiling point temperatures (T_S). The droplet diameter is fixed at 1.95±0.03mm. By adjusting the height between the syringe and surface, the impact velocity U_0 can be varied between 0.45 and 1.1 m/s, resulting the Weber number $We = \rho U_0^2 D_0/\sigma$, ranging from 20 to 70.

Table 1 Physical properties of the tested liquids at 1 atm and 20°C

Liquid	σ(N/m)	μ(mPa.s)	ρ(g/cm³)	boiling point (℃)
n-heptane	0.0204	0.41	0.680	98.4
n-decane	0.0243	0.92	0.730	174.2
n-tetradecane	0.0265	2.18	0.767	254.0

The surfaces used in this work are two stainless steel surfaces with different roughness. Figure 2 shows the scanning electron microscope (SEM) images of the surfaces. The surface roughness is R_a=0.1μm for the smooth surface and 5μm for the rough surface. The surface is heated from 30℃ to 500℃ in this work.
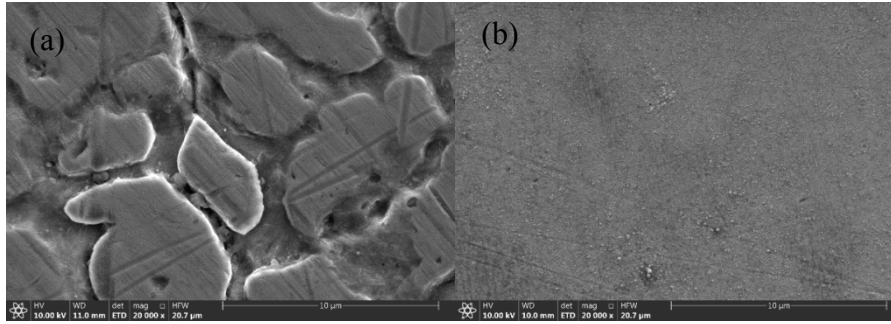
Figure 2 Scanning electron microscope (SEM) images of (a) the rough surface and (b) the smooth surface

The evaporation time is defined as the time from the impact of the droplet on the surface to the time when the droplet is fully evaporated. The evaporation time of n-heptane at $We \approx 20$ and 50 is presented in Figure 3. It takes shorter time for the droplet to completely evaporate at higher surface temperature (T_w) in evaporation and nucleate boiling regime. The droplet have shortest evaporation time in the critical heat flux point (T_C), which is 160℃ for n-heptane. Then the evaporation time is slightly increased as presented in the sub image in Figure 3(a) in the transition regime until the dynamic Leidenfrost temperature is reached (180℃ for n-heptane at $We \approx 20$ and 50). Figure 3(b) shows a schematic diagram about the droplet evaporation time at different wall temperature and regimes.
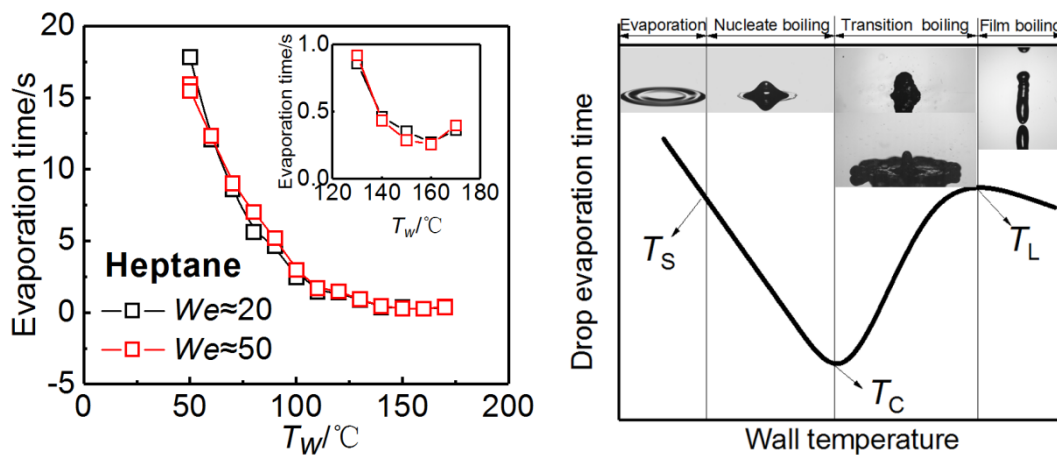

Figure 3 (a)Evaporation time of n-heptane droplet on heated surface at $We \approx 20$ and 50; (b)Different regimes for droplet impact on surface with varied T_w.

3. Results and discussion

3.1 Phenomenological description

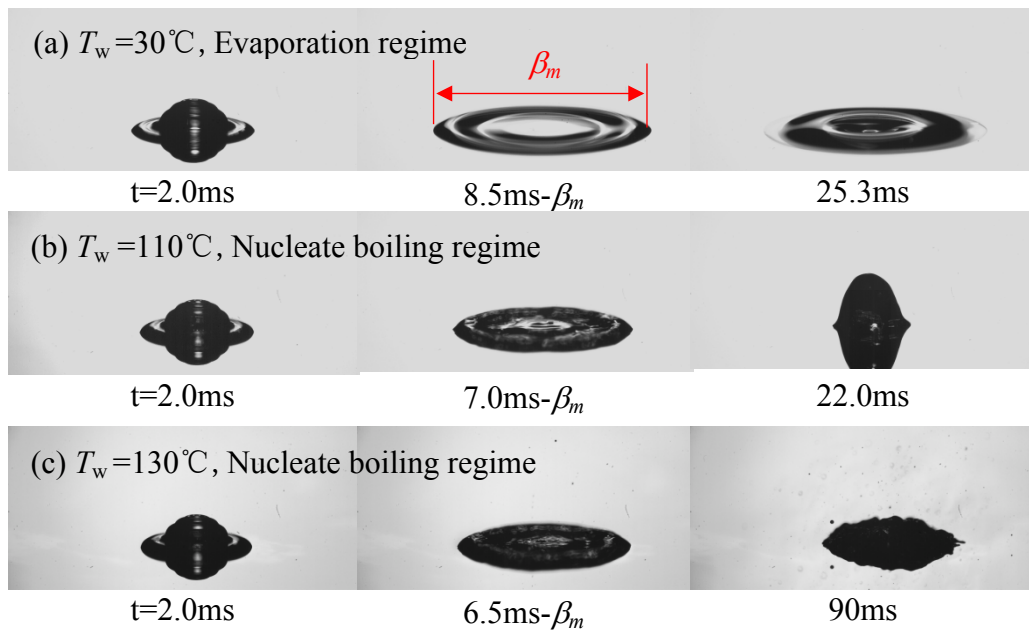### 3.1.1 Thermal hydrodynamic impact regions at various *We, Oh*, and roughness level

As a representative case, Figure 4 shows an n-heptane droplet impacting the heated smooth surface at $We \approx 20$. At a relatively small $T_w=30℃$, as seen in Figure 4(a), the droplet spreading is almost the same with that on a cold surface because the T_w is slightly higher than the environmental temperature so that the vaporization is minimal. The droplet reaches its maximum spreading diameter $\beta_m (\beta_m=D_m/D_0)$ at 8.5ms, and the lamella recoils afterwards. The recoil is promoted with the increase of T_w at $T_w=110℃$, as shown in Figure 4(b) at 25.3ms.

At $T_w=130℃$, which is higher than the boiling temperature $T_b=98℃$ of n-heptane, as shown in Figure 4(c), some bubbles are formed inside the droplet by nucleate boiling. Enlarged images of droplets at $We \approx 50$ where the bubbles in the droplet are more conspicuous are presented in Figure 7. Multiple secondary droplets are ejected from the droplet during its recoiling due to the high rate of heat transfer from the surface and consequent growth of vapor bubbles.

As we have discussed in Section 2, there is a critical surface temperature T_C at which the boiling is the strongest and the evaporation time is the shortest. It is found that $T_C =160ºC$ at $We \approx 20$ for n-heptane as already presented in Figure 3a. Further increase of the T_w weakens the boiling because the heat transfer enters the transition

boiling regime and large vapor bubbles are generated under the lamella as presented in Figure 4(d). It is noted that the contact angle is larger than 90° at 4.5ms, which indicates the wetting-to-non-wetting transition by increasing the T_w; this is a universal phenomenon for all the cases. Furthermore, due to the partial non-wetting and therefore less energy dissipation, the receding lamella gains more kinetic energy and forms a column, which tends to bounce away from the surface at 30ms.

At T_w=190℃ , which is higher than the dynamic Leidenfrost temperature T_L=180℃ for n-heptane at We≈20, as shown in Figure 4(e), film boiling occurs, and no secondary droplets were observed. This is because the formation of Leidenfrost gas cushion insulates heat transfer from the surface to the droplet. The droplet is supported by a developing vapor layer whose thickness is several orders of magnitude smaller than the droplet initial diameter[16], and it bounces off after a short period of time at 17.4ms defined as residence time.
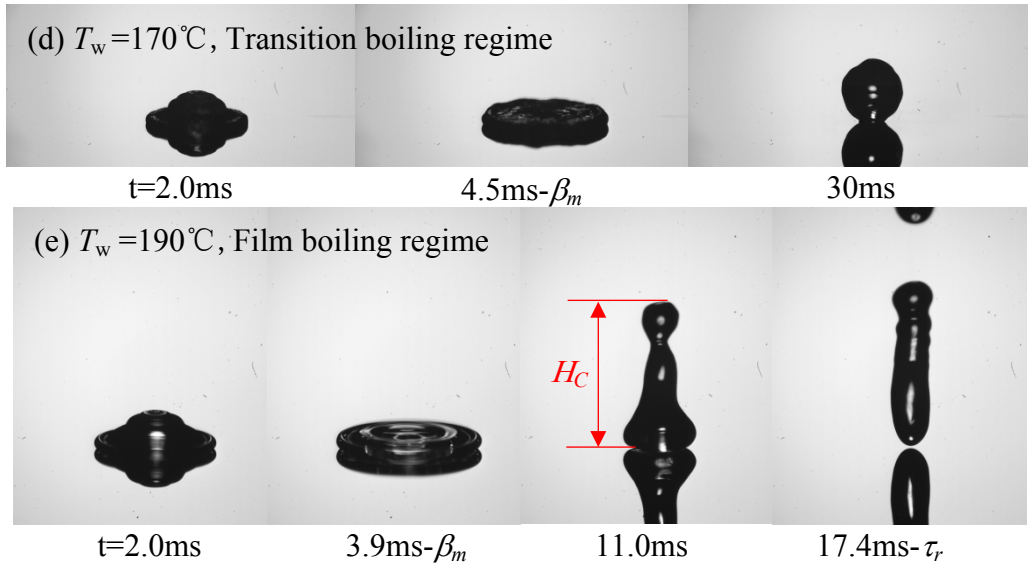

(a) T_w=30℃, Evaporation regime
β_m
t=2.0ms   8.5ms-β_m 25.3ms

(b) T_w=110℃, Nucleate boiling regime
t=2.0ms   7.0ms-β_m 22.0ms

(c) T_w=130℃, Nucleate boiling regime
t=2.0ms   6.5ms-β_m 90ms

(d) T_w =170℃, Transition boiling regime

t=2.0ms   4.5ms-β_m 30ms

(e) T_w =190℃, Film boiling regime

H_C

t=2.0ms   3.9ms-β_m 11.0ms   17.4ms-τ_r

Figure 4 Typical images of n-heptane droplets at We≈20 on smooth surface in different regime

Figure 5 shows images of n-heptane droplet at We≈20 impact on rough surface at T_w =170℃. Different from cases on smooth surface, the droplet has already reached film boiling regime on rough surface, the droplet bounces at 18ms after reaching the maximum spreading diameter at 3.8ms, which is a little bit longer compared to the residence time on smooth surface.

t=2.0ms   3.8-β_m 11.0ms   18.0ms-τ_r
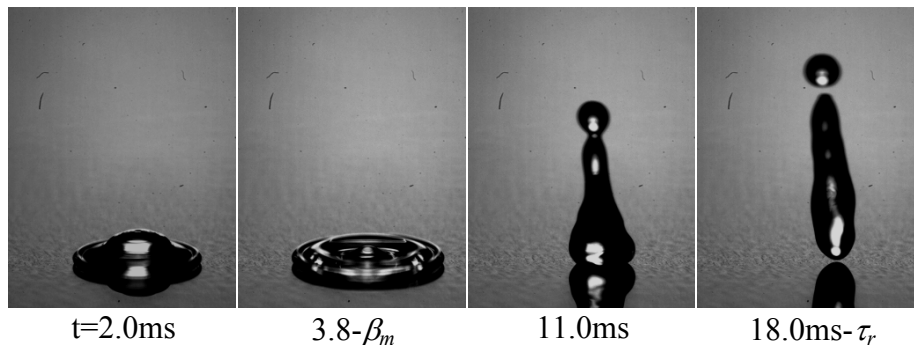
Figure 5 Typical images of n-heptane droplets at We=20 on rough surface at T_w =170℃.

3.1.2. Bubble formation at various We, Oh and roughness

When the T_w is higher than the liquid boiling point, isolated vapor bubbles are generated at the contact surface. Images of the bubbles formation in the n-heptane droplet impacting the smooth surface at We≈50 and T_w=110℃ are shown in Figure 6.

There are small bubbles generated in a circle because of the heating of the surface at 1.0ms by nucleate boiling as marked by a red arrow. A bubble in the center appears at 1.1ms because of the contact of air disk with the surface under the droplet [17] as marked by a red arrow. During the spreading, the part of the lamella with bubbles is thinner and evaporated faster at 7.8ms which looks like a wheel hub.
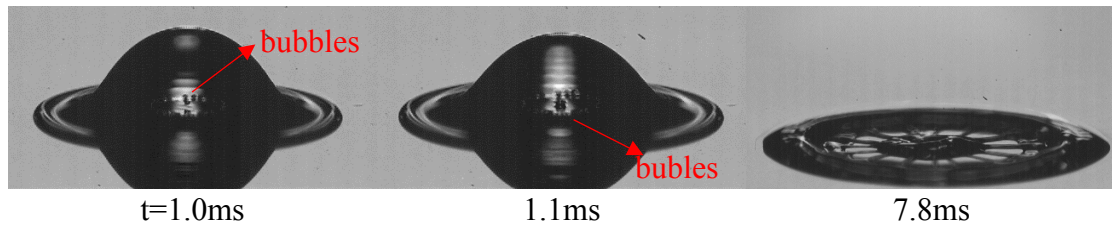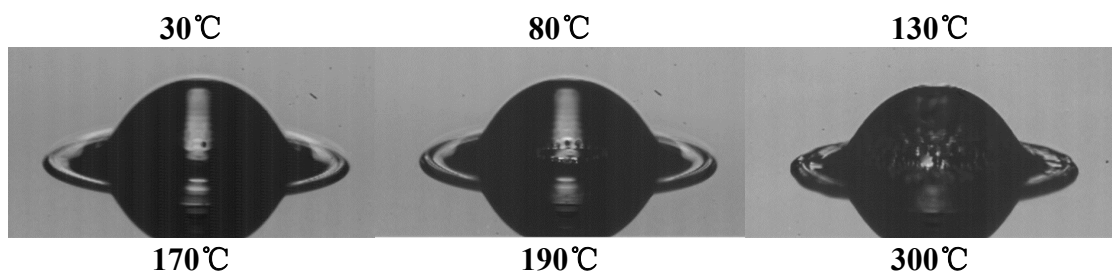

t=1.0ms   1.1ms   7.8ms

Figure 6 Enlarged images of bubbles formed in the n-heptane droplets during spreading at We≈50 at T_w=110℃.

Figure 7 shows the bubble formation of n-heptane at We≈50 and 1.0ms with different T_w. Firstly, images of the droplet at T_w=30℃ that with only one bubble formed in the middle because of the compress of the air disk [17] during the spreading is presented in Figure 7. At T_w=80℃, the n-heptane droplet reaches the boiling point, a circle formed by multiple small bubbles is observed. At T_w=130℃ and T_w=170℃, much more bubbles are formed because of higher heat transfer due to the increase of T_w. At T_w=190℃ and T_w=300℃ and, the droplet is in film boiling regime with no bubbles formed but a thin film under the droplet.

30℃   80℃   130℃
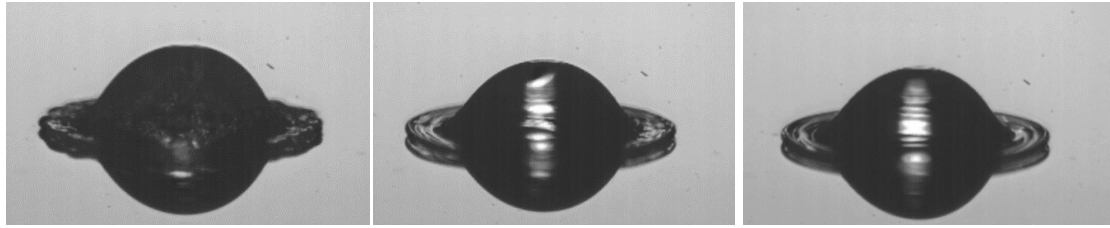

170℃   190℃   300℃

Figure 7 Enlarged images of bubbles formed in the n-heptane droplets during spreading at $We \approx 50$ at 1.0ms on heated surface with different T_w

Figure 8 shows bubble formation of n-tetradecane on smooth and rough surface at different T_w. At T_w=265℃, a circle of small bubbles formed because of heating at $T_w > T_S$ (the boiling point for n-tetradecane is 254℃) in nucleate boiling regime both on smooth surface and rough surface. Then at T_w=280℃, multiple bubbles are generated on rough surface while there is still only a circle of small bubbles formed on smooth surface. At T_w=310℃ and 330℃, multiple droplets with larger sizes are generated on smooth surface while much more bubbles are formed for droplet on rough surface. In conclusion, larger surface roughness provides more nucleate sites and leads to more and larger bubbles formed at the same time and T_w.
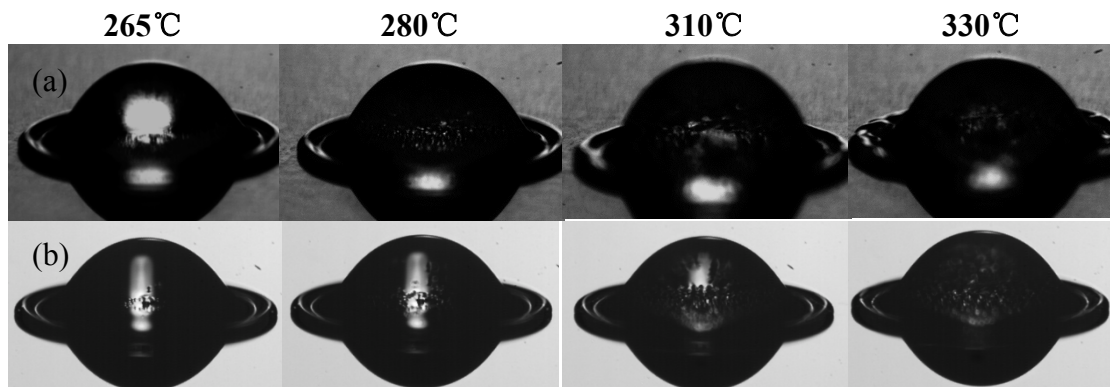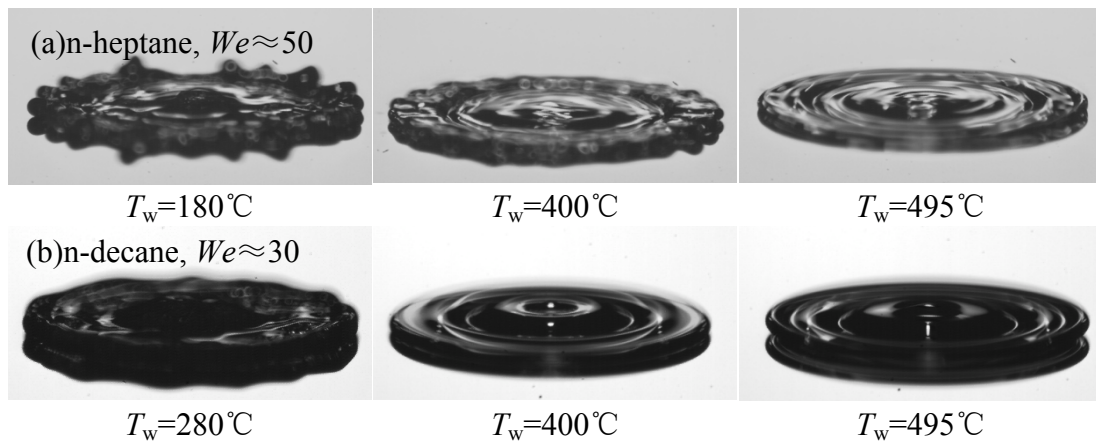

Figure 8 Enlarged images of bubbles formed in the n-tetradecane droplets during spreading on the roughness surface with different T_w at $We \approx 70$ at 0.9ms. (a)rough surface; (b)smooth surface.

3.1.3 Rim disturbance at various *We*, *Oh*, and roughness

Figure 9 shows images of n-heptane, n-decane and n-tetradecane droplet spreading on smooth and rough surface above Leidenfrost temperature at 3.0ms. For

n-heptane droplet as presented in in Figure 9(a), at T_w=180℃, different from that presented in Figure 4(e), finger-like disturbances were observed on the periphery of the lamella at 3.0ms. Previous literature has suggested that the fingering is triggered by the Rayleigh-Taylor instability of the decelerating contact line[18]. We found that the formation of the fingering pattern is first promoted because the gas density near the contact line is reduced due to an increase in T_w. Then, the increase in T_w results in the decrease of the total contact line length, and as such fingering formation is not favored as presented in Figure 9(a) at T_w=495℃. Consequently, the liquid is levitated completely by the Leidenfrost gas layer, and the fingering formation during the spreading process is mitigated due to the vanishment of the contact line. The rim of the lamella first spreads and then recedes over the Leidenfrost gas layer. Similar influence of T_w is also observed for n-decane and n-tetradecane on smooth and rough surface at varied We in Figure 9(b-d). Such fingering disturbance was also observed by Khavari et al.[19] before the transition boiling regime and it was found that the number of fingers increases with We and decreases with T_w.
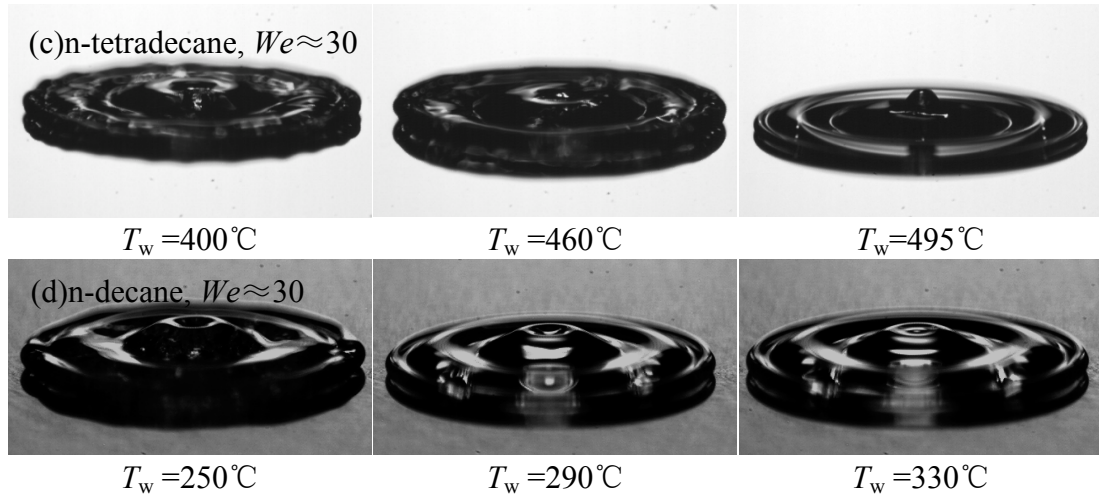

(a)n-heptane, $We≈50$
T_w=180℃ T_w=400℃ T_w=495℃

(b)n-decane, $We≈30$
T_w=280℃ T_w=400℃ T_w=495℃

(c)n-tetradecane, $We\approx30$		
T_{w} =400℃	T_{w} =460℃	T_{w}=495℃
(d)n-decane, $We\approx30$		
T_{w} =250℃	T_{w} =290℃	T_{w} =330℃

Figure 9 Images of rim disturbance of n-heptane, n-decane and n-tetradecane at varied We and T_{w} at t=3.0ms

3.2 Spreading dynamics and maximum spreading diameter

3.2.1 Spreading dynamics on varied T_{w} and roughness

Figure 10 shows the evolution of non-dimensional spreading diameter, $\beta=D(t)/D_{0}$, of n-heptane and n-tetradecane droplet impacting on smooth and rough surface with different T_{w}. For n-heptane droplet at $We\approx20$ impacting on smooth surface as presented in Figure 10(a), at T_{w} =30℃, the droplet is in evaporation regime, it spreads to a maximum spreading diameter denoted by β_{m} and slightly recoils because of its surface tension. At T_{w} =50℃, the droplet spreads more slowly and reaches a smaller β_{m}, starts recoils, and then vibrates. At T_{w} =80℃ and 100℃, the droplet is in the nucleate boiling regime, it reaches a smaller β_{m} and starts to vibrate later than it does in the evaporation regime because of larger recoils heights. At T_{w} =170℃, the droplet is in transition regime with lots of secondary droplets being ejected, the spreading diameter is not that smooth compared to that in evaporation and nucleate boiling regime. At T_{w} =190℃, 400℃ and 500℃, the droplet is in film

boiling regime, and it recoils quickly after reaching β_m and shows little difference in the evolution of β. Similar trends is also observed for n-heptane on rough surface as presented in Figure 10(b), except that the droplet has already in film boiling regime at 170℃. The time when the droplet reaches β_m is defined as τ_m as marked in Figure 10(b). The β evolution ends when the droplet is completely rebound from the surface at τ_r. The n-tetradecane droplet spreading on smooth and rough surfaces is presented in Figure 10(c)(d), the droplet vibrates in nucleate boiling and transition boiling regime.
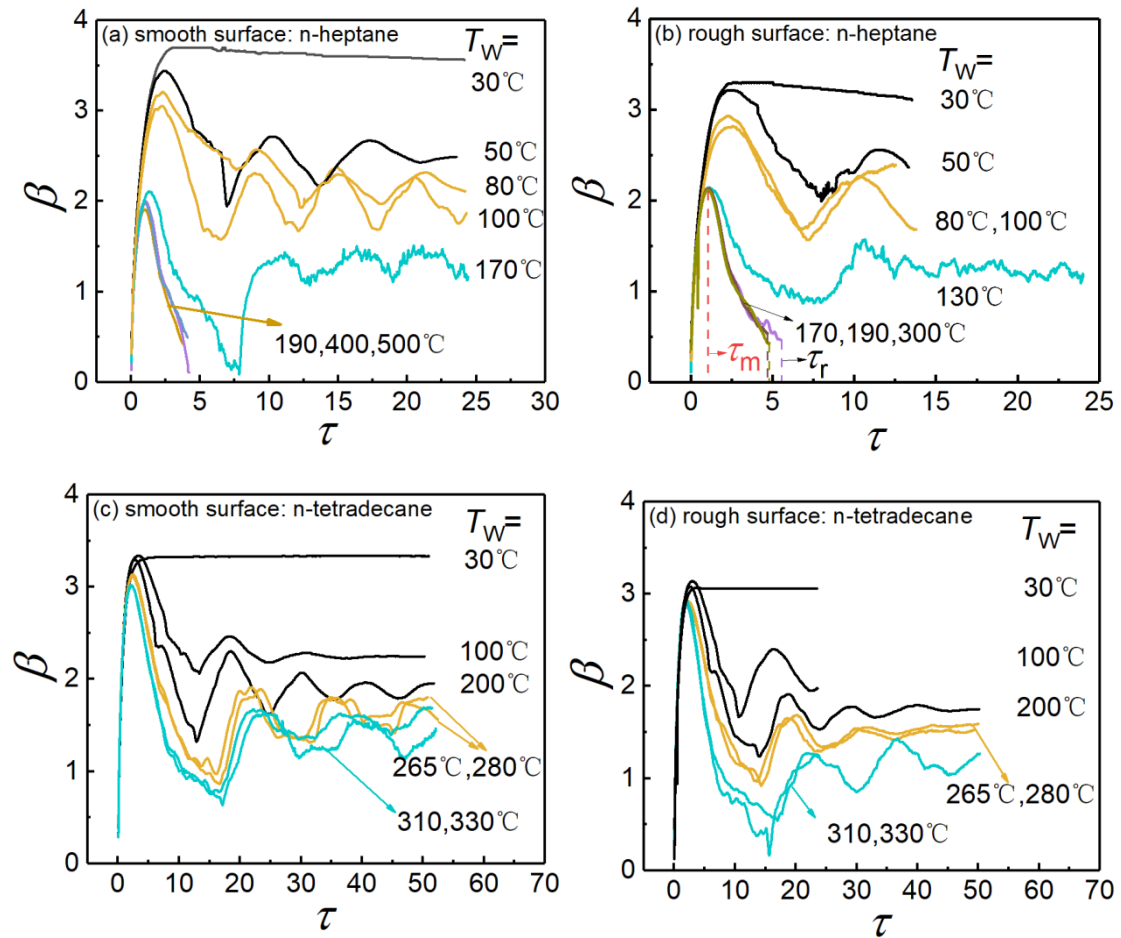

Figure 10 Non-dimensional spreading diameter of (a) n-heptane droplet at $We≈20$ on smooth surface; (b) n-heptane at $We≈20$ on rough surface; (c)n-tetradecane at $We≈70$ on smooth surface; (d) n-tetradecane at $We≈70$ on rough surface.

3.2.2 Maximum spreading diameter

The non-dimensional maximum spreading diameter of the spreading lamella, β_m, is one of the prominent parameters to describe the morphology of an impacting drop. Figure 11(a) shows the variation of β_m of n-heptane droplets with T_w at different We on smooth surface. Overall, β_m increases with We from 20 to 70 at different T_w; it decreases with increasing T_w until reaches the film boiling regime, where β_m is not strongly influenced by T_w. It is noted that the Leidenfrost temperature marked by the dash line in the present We range s barely changed, which is consistent with the finding in literature[20]. The β_m for n-heptane at $We \approx 70$ is slightly increased with increasing T_w in the film boiling regime, which is due to the significant .

When the surface is not heated, β_m is larger for liquids with smaller viscosity on smooth surface, as shown in Figure 11(b), because of less viscous dissipation during the spreading. Then β_m decreases with the increase of T_w until it reaches a Leidenfrost temperature T_L. The n-heptane, n-decane and n-tetradecane droplets reach T_L at T_w=180, 260, and 380℃ respectively. The n-heptane droplet has largest β_m when the surface is not heated, thus is mostly influenced by the T_w since three liquids eventually reaches the same β_m at $T_w > T_L$.
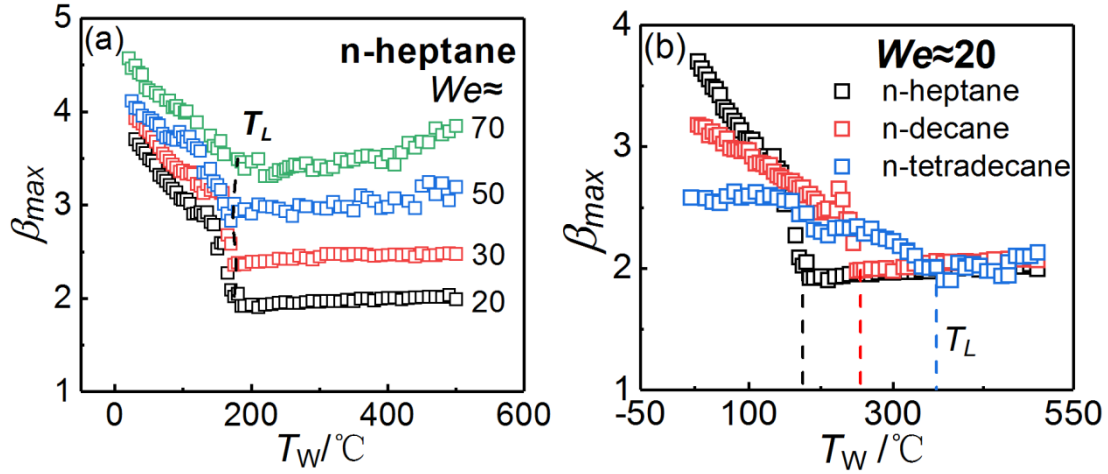
Figure 11 (a)β_m of n-heptane at varied T_w and We on smooth surface; (b) β_m of n-heptane, n-decane and n-tetradecane at varied T_w at $We \approx 20$ on smooth surface.

It is well known that surface roughness reduces β_m when the surface is not heated because of larger energy dissipation during the spreading[21]. Figure 12 represents β_m of n-heptane droplets on rough and smooth surfaces at $We \approx 20$. It is seen that surface roughness also influences the spreading of droplets on a heated surface. Firstly, the droplet spreading is smaller on rough surface at $T_w < T_L$ mainly because of larger viscous dissipation during the spreading as discussed comprehensively in the literature [21]. It is noted that the droplet reaches T_L earlier on the rough surface and has a larger β_m. A possible explanation is that the cavity in the roughness provides more space for fuel vapor, and it is easier to form a vapor layer to levitate the droplet than the smooth surface, consequently resulting in a larger β_m. The lower Leidenfrost temperature for a rough surface is due to the increase of nucleation sites provided by surface roughness.
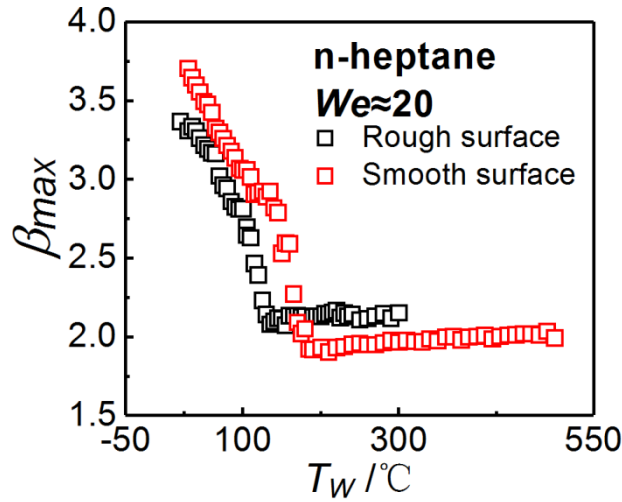
Figure 12 β_m for n-heptane droplets at smooth surface and rough surface at $We\approx20$.

The maximum spreading diameter is approximately the same in the film boiling regime as presented in Figure 11 which is also strongly concerned with multiple models to predict. As shown in Figure 13, three typical models for β_m of droplet impact on heated surface in film boiling regime are compared with the data in this work[22]. Clearly, the data in this work lies in $\sim We^{0.3}$, which is consist of the prediction in previous scaling law [10, 23].
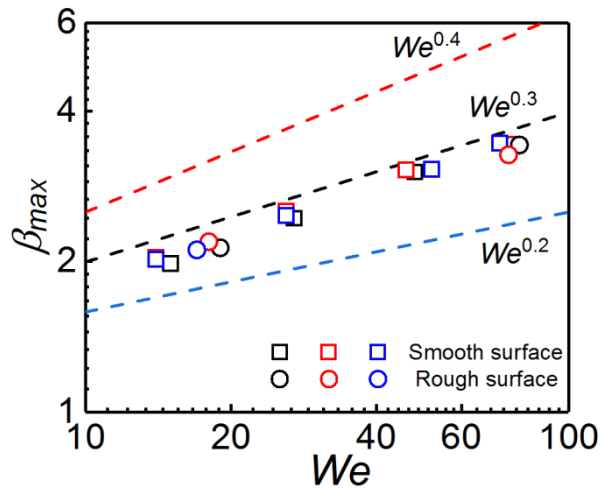

Figure 13 correlations of β_m in film boiling regime from different models[22].
Black symbols: n-heptane; red symbols: n-decane; blue symbols: n-tetradecane.

3.3 Droplet bouncing in film boiling regime

3.3.1 Bouncing height

When the droplet reaches the film boiling regime, the non-dimensional spreading diameter β shown in Figure 10 is barely changed. Figure 14 shows the non-dimensional height of the droplet center $H_c{}'$ ($H_c U_0/D_0$) during the rebound in the film boiling regime with varied T_w at varied We on smooth and rough surface. With the increase of T_w, the higher vapor pressure makes the droplet rebound faster and increase $H_c{}'$ at the same time as presented in Figure 14(a). Larger We leads to larger β_m as presented in Figure 11, and takes a longer time for the droplet to rebound as shown in Figure 14(b), which has also been observed by Gastanet et al.[8].

For liquids with varied viscosity, although they have almost same β_m when the droplet reaches T_L in film boiling regime as presented in Figure 11, the n-tetradecane with larger viscosity still rebound slower than n-heptane with smaller viscosity as shown in Figure 14(c). The droplet is inertial driven during the spreading which is barely influenced by viscosity. Viscosity begins to play a role during the rebound driven by capillary pressure and consequently a higher viscosity results in slower rebound and smaller central height at the same time. The surface roughness slightly influences β_m as presented in Figure 12 and also slightly effect $H_c{}'$ as shown in Figure 14(d).
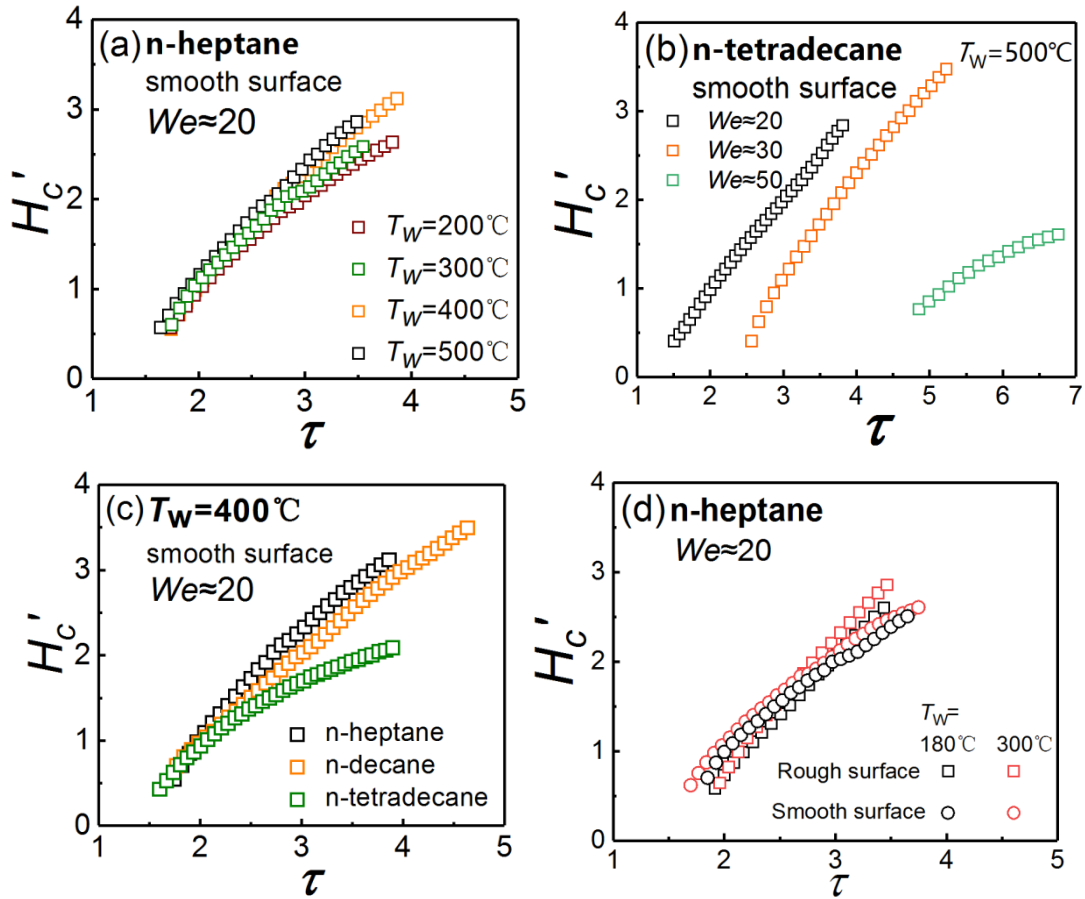
Figure 14 Non-dimensional droplet central height $H_c' = H_c U_0/D_0$ for (a)n-heptane at $We \approx 20$ on smooth surface at varied T_w; (b)n-tetradecane at T_w=500℃ on smooth surface at varied We; (c)n-heptane, n-decane and n-tetradecane at T_w=400℃ on smooth surface at $We \approx 20$; (d)n-heptane on smooth and rough surface at $We \approx 20$ at T_w=180 and 300℃.

3.3.2 Residence time

Figure 15(a) shows the non-dimensional residence time $\tau_r = t_r U_0/D_0$ for n-tetradecane at varied T_w and We on smooth surface. It takes a shorter time for the droplet to rebound when We is small. It is noted that most previous studies assumed that residence time is only related to We[14, 24, 25]. However, τ_r is found to be also influenced by liquid viscosity as shown in Figure 15(b) and surface roughness in Figure 15(c). It takes a longer time to rebound for liquids with larger viscosity on surface with larger roughness.
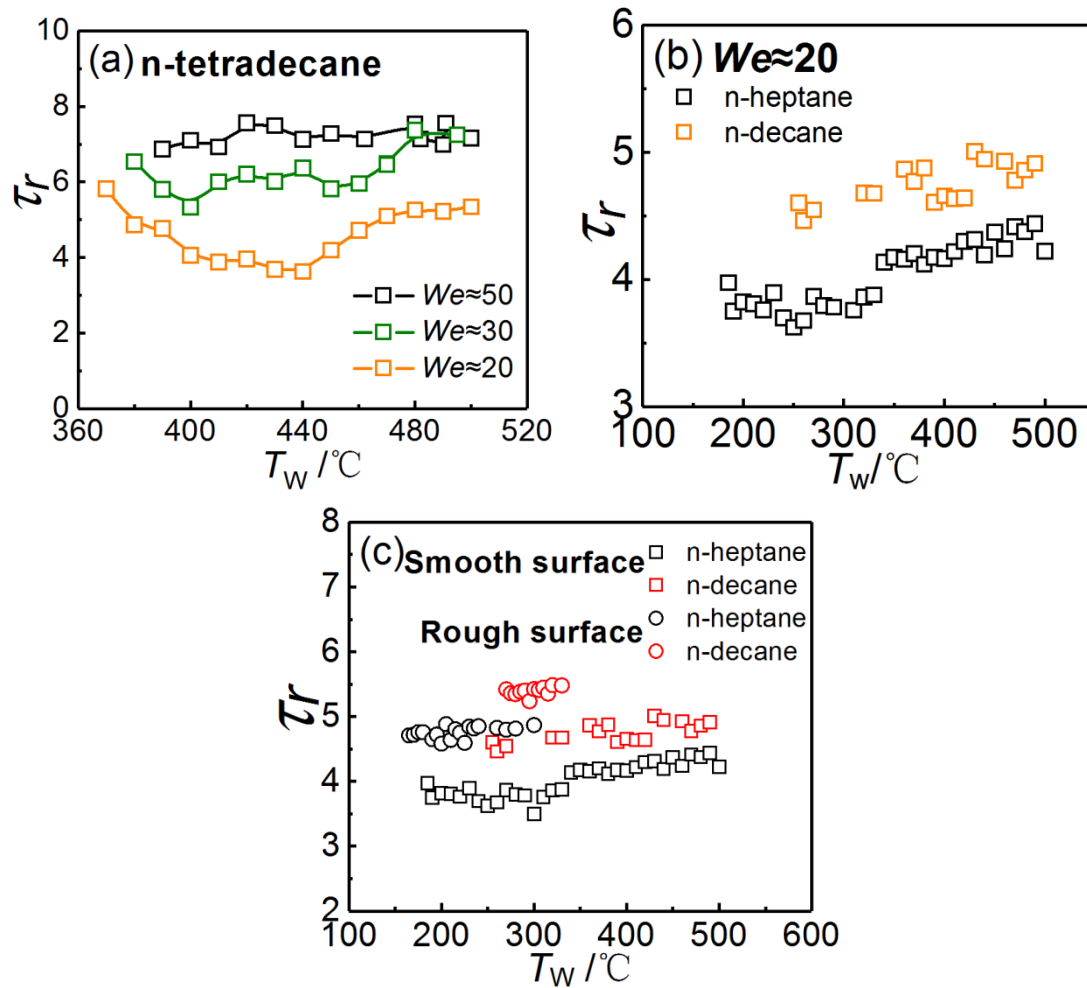
Figure 15 (a)Non-dimensional residence time $\tau_r=t_r U_0/D_0$ for n-tetradecane at varied T_w and *We* on smooth surface; (b)τ_r for different liquids at varied T_w; (c)τ_r for n-heptane and decane with varied T_w on smooth and rough surface.

To understand the experimental observations, we divided the residence time τ_r to the time duration for reaching β_m and that for recoil as shown in Figure 16(a). It turns out that the droplet takes the same time to spread to the same β_m but different times to recoil. The droplet dynamics is dominated by impact inertia during the spreading because of the large Reynolds number, and therefore it shows no difference with a vapor layer underneath to prevent the contact with the surface. But viscosity begins to play a role during the rebound driven by capillary pressure, and consequently a higher viscosity eventually results in a larger residence time τ_r.

We also analyzed the residence time for different surface roughness in Figure 16(b), which shows that the difference also roots in the recoil stage. All these results suggest that both surface roughness and liquid viscosity affect the residence time of the bouncing droplet and need to be considered in modeling.
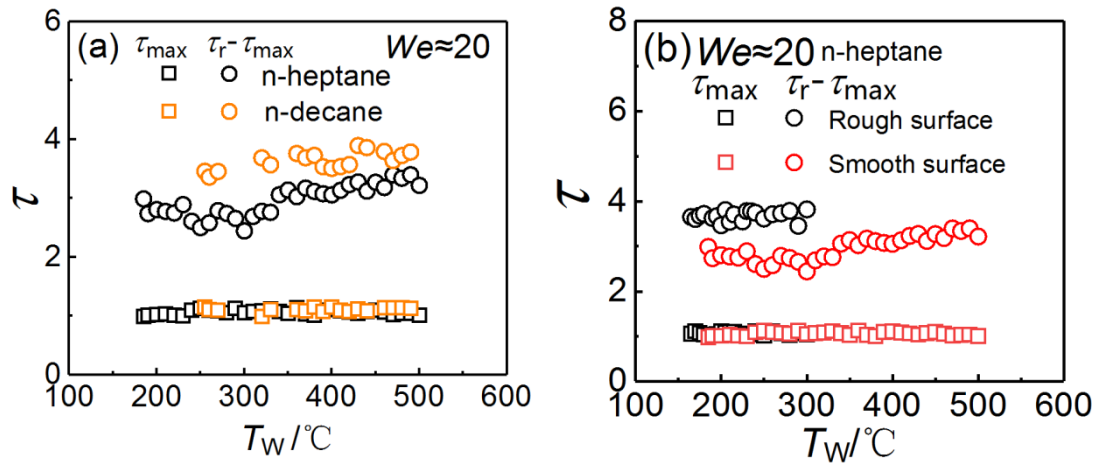

Figure 16 (a) Non-dimensional maximum spreading time τ_{max}(square) and recoil time (circle) for n-heptane and n-decane. (b) Non-dimensional maximum spreading time τ_{max}(square) and recoil time (circle) for n-heptane droplet on rough and smooth surface

Above all the discussion about spreading and rebound process, residence time τ_r is strongly concerned with multiple models to predict [14, 24, 25]. As shown in Figure 17, the resident time is influenced by the liquid viscosity and surface roughness, thus the models that don't contain liquid viscosity and surface roughness will not be able to give good prediction. Such comparison indicates that liquid viscosity and surface roughness should be considered in residence time modeling in the future work.
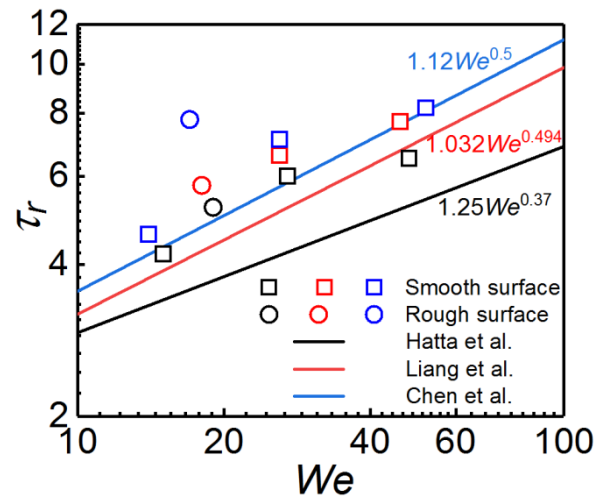
Figure 17 correlations of τ_r from different models. Hatta et al.[14]: $\tau_r \sim 1.25We^{0.37}$; Chen et al.[24]: $\tau_r \sim 1.12We^{0.5}$; Liang et al. [25]: $\tau_r \sim 1.032We^{0.494}$. Black symbols: n-heptane; red symbols: n-decane; blue symbols: n-tetradecane.

4. Conclusion

With the increasing interest in engine downsizing and in considering the strong relation between the spray impingement and droplet-solid surface interaction, we have comprehensively investigated the thermo hydrodynamic behaviors of droplet impact on solid surface. The particular emphasis of the study was on the effect of droplet viscosity, the surface roughness and temperature on droplet spreading and bouncing, bubble generation, spreading rim disturbance and the spreading and bouncing dynamics.

1. Four typical regimes of droplet impact on heated surface are identified. Bubbles generated inside the droplet at $T_w > T_b$ are observed, more and larger bubbles are generated with increasing T_w in nucleate boiling and transition boiling regime. No bubbles are formed in film boiling regime. The rim is smoother with weaken rim disturbance with the increase of T_w.

2. The droplet oscillates in terms of spreading and contracting for $T_L > T_w > T_b$, as

identified by the spreading diameter (β) vibration as a function of time. However, for $T_\mathrm{w} > T_\mathrm{L}$, the β evolution shows barely difference in film boiling regime. The maximum non-dimensional diameter β_{max} decreases with increasing T_w until a dynamic Leidenfrost temperature T_L is reached. The liquid viscosity decreases β_{max} when the surface is not heated and shows no effect in film boiling regime.

3. Liquids with larger viscosity takes larger time to recoil and eventually result in larger residence time τ_r. The residence time is significantly influenced not only by Weber number, but also by liquid viscosity and surface roughness, which should be considered in future model of residence time.

The present results are expected to provide useful guidance in the development of spray dynamic models and the design of next-generation, down-sized engines.

Acknowledgement

Reference

[1] S. Chandra, C.T. Avedisian, On the collision of a droplet with a solid surface, Proceedings of the Royal Society A: Mathematical, Physical and Engineering

Sciences, 432(1884) (1991) 13-41.

[2] J.D. Bernardin, C.J. Stebbins, I. Mudawar, Mapping of impact and heat transfer regimes of water drops impinging on a polished surface, International Journal of Heat Mass Transfer, 40(2) (1997) 247-267.

[3] J.D. Naber, P.V. Farrell, Hydrodynamics of droplet impingement on a heated surface, SAE Transactions, (1993) 1346-1361.

[4] A.L.N. Moreira, A.S. Moita, M.R. Panão, Advances and challenges in explaining fuel spray impingement: How much of single droplet impact research is useful?, Progress in Energy and Combustion Science, 36(5) (2010) 554-580.

[5] V. Bertola, An impact regime map for water drops impacting on heated surfaces, International Journal of Heat and Mass Transfer, 85 (2015) 430-437.

[6] T. Tran, H.J. Staat, A. Prosperetti, C. Sun, D. Lohse, Drop impact on superheated surfaces, Phys Rev Lett, 108(3) (2012).

[7] A.-l. Biance, F. Chevy, C. Clanet, G. Lagubeau, D. Quéré, On the elasticity of an inertial liquid shock, Journal of Fluid Mechanics, 554 (2006) 47.

[8] G. Castanet, O. Caballina, F. Lemoine, Drop spreading at the impact in the Leidenfrost boiling, Physics of Fluids, 27(6) (2015).

[9] S. Fukuda, M. Kohno, K. Tagashira, N. Ishihara, S. Hidaka, Y. Takata, Behavior of small droplet imping on a hot surface, Heat Transfer Engineering, 35(2) (2013) 204-211.

[10] T. Tran, H.J.J. Staat, A. Susarrey-Arce, T.C. Foertsch, A. van Houselt, H.J.G.E. Gardeniers, A. Prosperetti, D. Lohse, C. Sun, Droplet impact on superheated micro-structured surfaces, Soft matter, 9(12) (2013).

[11] P. Zhao, G.K. Hargrave, H.K. Versteeg, C.P. Garner, B.A. Reid, E.J. Long, H. Zhao, The dynamics of droplet impact on a heated porous surface, Chemical Engineering Science, 190 (2018) 232-247.

[12] E.-S.R. Negeed, M. Albeirutty, S.F. Al-Sharif, S. Hidaka, Y. Takata, Dynamic behavior of a small water droplet impact onto a heated hydrophilic surface, Journal of Heat Transfer, 138(4) (2016).

[13] R.-H. Chen, S.-L. Chiu, T.-H. Lin, On the collision behaviors of a diesel drop impinging on a hot surface, Experimental Thermal and Fluid Science, 32(2) (2007) 587-595.

[14] N. Hatta, H. Fujimoto, K. Kinoshita, H. Takuda, Experimental study of deformation mechanism of a water droplet impinging on hot metallic surfaces above the leidenfrost temperature, Journal of Fluids Engineering, 119(3) (1997) 692.

[15] W. Zhang, T. Yu, J. Fan, W. Sun, Z. Cao, Droplet impact behavior on heated micro-patterned surfaces, Journal of Applied Physics, 119(11) (2016).

[16] L.R. Villegas, S. Tanguy, G. Castanet, O. Caballina, F. Lemoine, Direct numerical simulation of the impact of a droplet onto a hot surface above the Leidenfrost temperature, International Journal of Heat and Mass Transfer, 104 (2017) 1090-1109.

[17] S. T. Thoroddsn, T. G. Etoh, K. Takehara, N. Ootsuka, Y. Hatsuki, The air bubble entrapped under a drop impacting on a solid surface, Journal of Fluid

Mechanics, 545(545) (2005) 203-212.

[18] C. Josserand, S.T. Thoroddsen, Drop Impact on a Solid Surface, Annual Review of Fluid Mechanics, 48(1) (2016) 365-391.

[19] M. Khavari, C. Sun, D. Lohse, T. Tran, Fingering patterns during droplet impact on heated surfaces, Soft Matter, 11(17) (2015) 3298-3303.

[20] H.J.J. Staat, T. Tran, B. Geerdink, G. Riboux, C. Sun, J.M. Gordillo, D. Lohse, Phase diagram for droplet impact on superheated surfaces, Journal of Fluid Mechanics, 779 (2015).

[21] C. Tang, M. Qin, X. Weng, X. Zhang, P. Zhang, J. Li, Z. Huang, Dynamics of droplet impact on solid surface with different roughness, International Journal of Multiphase Flow, 96 (2017) 56-69.

[22] G. Liang, I. Mudawar, Review of drop impact on heated walls, International Journal of Heat and Mass Transfer, 106 (2017) 103-126.

[23] H. Nair, H.J. Staat, T. Tran, A. van Houselt, A. Prosperetti, D. Lohse, C. Sun, The Leidenfrost temperature increase for impacting droplets on carbon-nanofiber surfaces, Soft matter, 10(13) (2014) 2102-2109.

[24] R.H. Chen, S.-L. Chiu, T.-H. Lin, Resident time of a compound drop impinging on a hot surface, Applied Thermal Engineering, 27(11-12) (2007) 2079-2085.

[25] G. Liang, S. Shen, Y. Guo, J. Zhang, Boiling from liquid drops impact on a heated wall, International Journal of Heat and Mass Transfer, 100 (2016) 48-57.